Tectono-geochemistry analyses of fault rocks in shear zone of metamorphic core complex in north Jiangxi, China*

SUN Yan[1]**, SHU Liangshu[1], GUO Jichun[1], ZHU Wenbin[1], ZHANG Xihui[1], CHEN Xiangyun[2], WANG Feng[1] and FAURE M[3]

(1. Department of Earth Sciences, State Key Laboratory for Research of Mineral Deposits, Nanjing University, Nanjing 210093, China; 2. Bureau of Geology and Mineral Resources of Jiangxi, Nanchang 330002, China; 3. Department of Earth Sciences, Orleans University, Orleans 45067, France)

Received October 21, 2002; revised December 20, 2002

Abstract Through a systematic sampling test and mass equilibrium analysis of the three sorts of complex assemblages (intrusive complex, tectonic complex and metamorphic complex) penetrating the metamorphic core complex (MCC) in the Xingzi area of north Jiangxi, the authors find that, like major elements, the trace elements of small ion radius, big specific gravity and high potential form the accumulative series in fault rocks, instead of divergence series. In rare earth elements, ΣREE and HREE are relatively centralized, characteristic of rising and Eu loss in the distribution pattern. Only on the upside of the ductile fault, there exist some phenomena contrary to the general rules, most of which are restricted by the rock rheologic differentiation, coupling of mechanics and chemistry, and inversion of tectonic regime.

Keywords: tectonic complex, ductile shear zone, trace elements, rare earth elements, rock-rheology, tectonic inversion.

In the early 1980s, the metamorphic core complex study was started and its model of extensional tectonics was established[1]. To the year 1993 when the academic conference was held in France on "The Late Extension of the Orogenic Belt", the studies on the genesis classification and evolving process of metamorphic core complex (MCC) were further discussed[2]. Since the 1990s, cooperative studies on the metamorphic core complex have been carried out by Chinese and American geologists in north China[3], and by Chinese and French Scientists in south China[4]. During the course of study, the latter group found that, in the regions of Jiangxi-Hunan-Hubei, all the central parts of the MCC have intrusive rocks, which also occurred in the MCC of the Euro-American regions such as the central massif in France. Thus a term of intrusive metamorphic core complex (IMCC) was developed. In the complicated lithologic assemblage of IMCC, there are three sorts of complex composites from the core to the margin, which are intrusive complex, tectonic complex, and metamorphic complex. In the late period of the major orogenic movement, the most active portions for the dome extensional tectonic stress field and the geochemical field are tectonic complex belts. In general, the mylonite (inclusive of proto-mylonite and ultra-mylonite), gneissic mylonite (mylonitic gneiss) are typical fault rocks in the ductile zone.

Since the 1990s, new research achievements have been made worldwide on the subjects of the boundary migration of mylonitic grains in ductile shear zones of varied crystal depths and layers, mineral lattice differentiation, the increase and decrease of rock and mineral volumes, the assemblage and divergence of elements[5~7]. Much attention was focused on major element analyses in the course of tectono-geochemistry study in the ductile shear zone. A systematic test (Tables 1~3) and mass equilibrium analysis (Table 4) of lithologic sections (Fig. 1) from the three sorts of complexes penetrating Donggushan to Wenling in the Xingzi area of north Jiangxi are carried out in this study. In addition, a brief description is given on the variation of the trace elements and rare earth elements in the ductile shear mylonitic zone.

* Supported by the National Natural Science Foundation of China (Grant Nos. 40173001 and 40172067) and the State Key Laboratory of Oil/Gas Reservoir Geology and Exploration

** To whom correspondence should be addressed. E-mail: sunyan03@163.com

Table 1. Whole rock analyses from ductile shear zone of the Xingzi metamorphic core complex, northern Jiangxi ($\omega/10^{-2}$)[a]

Sample No.	Rock type	SiO_2	Al_2O_3	Fe_2O_3	FeO	TiO_2	CaO	MgO	K_2O	Na_2O	P_2O_5	MnO	LOS	Total
LS10	Mica schist	49.32	14.93	2.21	8.21	1.22	11.14	7.89	0.27	1.88	0.12	0.21	1.92	99.32
LS13	Mylonite	70.84	12.94	0.66	4.33	0.72	1.94	1.37	2.16	3.37	0.16	0.14	1.32	99.95
LS14	Mylonite	69.39	15.10	2.47	2.13	0.58	0.043	1.04	5.00	0.17	0.047	0.14	3.22	99.84
LS15	Gneissic mylonite	73.84	12.72	1.14	1.48	0.26	0.98	0.36	4.80	3.32	0.067	0.072	1.13	100.17
LS16	Gneiss	76.74	13.66	0.96	0.95	0.069	0.05	0.31	4.21	0.30	0.052	0.061	2.65	100.01
LS18	Fine granite	71.73	14.19	0.34	1.24	0.20	1.56	0.44	4.24	4.22	0.12	0.10	1.88	100.26

a) Analysed by Qi Liang, Open Laboratory of Ore Deposit Geochemistry, Institute of Geochemistry, Chinese Academy of Sciences, Guiyang.

Table 2. Trace element abundance from ductile shear zone of the Xingzi metamorphic core complex, northern Jiangxi ($\times 10^{-6}$)[a]

Sample No.	Rock type	Ba	Cu	Nb	V	Be	Ga	Ni	Zn	Co	Li	Pb	Cr	Mo	Sr
LS10	Mica schist	1837	71.07	84.16	421.0	0.2078	15.07	67.45	549.8	44.57	136.1	19.09	300.2	5.525	112.6
LS13	Mylonite	738.4	14.2	18.2	111.3	2.437	28.48	22.61	189.7	18.98	191.0	32.89	63.18	3.178	177.6
LS14	Mylonite	862.1	21.86	98.78	85.72	9.711	62.44	23.91	587.0	15.65	434.9	33.85	60.82	3.910	11.71
LS15	Gneissic mylonite	927.2	17.01	16.03	45.52	1.748	31.03	7.973	178.3	6.515	121.8	11.19	12.60	3.533	45 71
LS16	Gneiss	512.2	6.063	50.43	36.96	4.034	61.66	6.255	217.1	3.086	357.3	25.26	10.02	2.928	8.625
LS18	Fine granite	1300	19.59	20.84	46.88	3.476	35.30	8.435	241.6	5.810	79.59	36.54	12.48	3.223	176.2

a) Analyzed by Qi Liang, Open Laboratory of Ore Deposit Geochemistry, Institute of Geochemistry, Chinese Academy of Sciences, Guiyang.

Table 3. REE compositions from ductile shear zone of the Xingzi metamorphic core complex, northern Jiangxi ($\times 10^{-6}$)[a]

Sample No.	LS10	LS13	LS14	LS15	LS16	LS18
Rock type	Mica schist	Mylonite	Mylonite	Gneissic mylonite	Gneiss	Fine granite
La	3.561	26.7	44.29	20.23	0.675	35.49
Ce	10.28	59.79	46.04	49.69	1.491	61.66
Pr	2.018	5.639	9.33	4.568	0.3586	4.307
Nd	6.177	19.96	35.42	15.79	0.6258	14.29
Sm	2.38	5.425	9.001	4.493	0.2275	2.963
Eu	0.8737	1.162	1.538	0.7195	0.0307	0.6195
Gd	3.293	5.528	7.139	4.626	0.2053	2.008
Tb	0.6517	1.077	1.463	0.9412	0.1193	0.4281
Dy	3.828	5.588	4.715	5.046	0.234	1.193
Ho	0.8159	1.161	0.9421	1.093	0.0727	0.2566
Er	2.557	3.446	2.631	3.644	0.1813	0.6361
Tm	0.3807	0.5405	0.4572	0.5738	0.0528	0.138
Yb	2.077	2.723	2.378	3.168	0.1831	0.4802
Lu	0.3554	0.4405	0.4222	0.5128	0.0368	0.0781
Y	22.6	32.47	25.84	31.79	1.202	5.65
ΣREE	61.7424	171.65	191.9663	146.8845	4.4939	130.1126
HREE/LREE	1.394	0.541	0.355	0.673	1.047	0.142
Eu/Eu^*	0.964	0.649	0.572	0.483	0.430	0.740
La/Yb	1.132	6.475	12.298	4.217	2.435	48.795

a) Analyzed by Qi Liang, Open Laboratory of Ore Deposit Geochemistry, Institute of Geochemistry, Chinese Academy of Sciences, Guiyang.

1 Mass equilibrium analysis

When the mylonite and its components of the primary rocks are identified, the migration contrast in it is to be conducted under certain confined conditions. The mass equilibrium analysis is to be conducted on the fault rocks in the shear zone in Fig. 1 by component conservation of ordinary Al_2O_3[8,9].

(1) From Table 4 and Fig. 2, the component migration of mica schist (LS10) to mylonite (LS14) can be found. Under Al_2O_3 component conservation, assuming m_o as the proto-rock mass, and m_A as the mass after mylonitization, the ratio of them is $m_o/m_A = 1.014$. If the new added mass is Δm, and the added mass for certain component is Δm_i for the ith component, the concentration relationship of pre- and

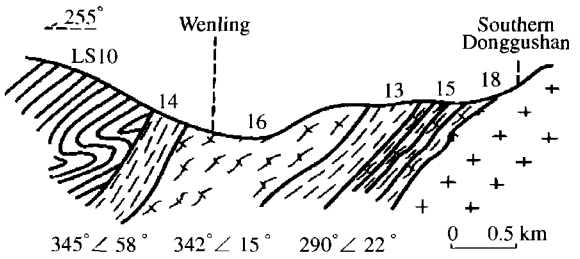

Fig. 1. Lithologic profile in ductile shear zone in Xingzi area of northern Jiangxi. LS10, Number of samples, middle Proterozoic mica schist of Shuangqiao Group; LS14, mylonite; LS16, gneiss; LS13, mylonite; LS15, gneissic mylonite; LS18, fine granite.

post-mylonitization is $C_i = m_o/m_A\,(C_i^o + \Delta C_i)$, where C_i^o is a certain component concentration of the proto-rocks, C_i is the component concentration of post mylonitization, that is, $\Delta C_i = \Delta m_i/m_o$. The mass iso-proportion line of $C_i = 1.014\ C_i^o$ will be further determined to be a beeline with a slope as m_o/m_A, corresponding to $C_i = C_i^o$ in conservations of mass and volume. The following is the migration of the components of mylonite: the bring-in of SiO_2, Fe_2O_3 and K_2O is evident in major elements; Ga, Nb, Be, Y and La are increased in the trace elements and rare earth elements (Fig. 2).

Table 4. Mass equilibrium calculation analysis of fault rocks in ductile shear zone of the Xingzi metamorphic core complex, northern Jiangxi

Rock sample No.	Mica schist → mylonite		Fine granite → Gneissic mylonite		Gneissic mylonite → mylonite	
	LS10	LS14	LS18	LS15	LS15	LS13
m_o/m_A	1.014		0.896		1.017	
Composition	$\Delta C_i/C_i^o$	$\Delta m_i/m_o$	$\Delta C_i/C_i^o$	$\Delta m_i/m_o$	$\Delta C_i/C_i^o$	$\Delta m_i/m_o$
SiO_2	39.16	19.32	14.89	10.68	-5.67	-4.18
Fe_2O_3	10.54	0.23	274.21	0.93	-43.07	-0.49
FeO	-74.33	-6.10	33.21	0.41	187.68	2.78
TiO_2	-52.98	-0.64	45.09	0.09	172.29	0.45
CaO	-99.62	-11.10	-29.89	-0.46	94.65	0.93
MgO	-86.96	-6.86	-8.69	-0.04	274.19	0.99
K_2O	1731.32	4.68	26.35	1.12	-55.75	-2.68
Na_2O	-91.06	-1.71	12.20	-0.51	0.00	-0.01
P_2O_5	61.26	-0.07	-37.69	-0.05	134.81	0.09
MnO	-34.06	-0.07	-19.64	-0.02	91.19	0.07
LoS	65.88	1.36	-32.92	-0.62	13	0.17
Total		0.96		11.53		-1.87

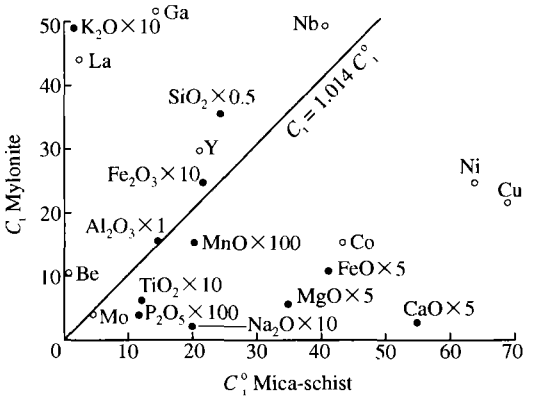

Fig. 2. Mass iso-proportion line of mylonite in ductile shear zone—the proportion of mylonite (LS14) with mica schist (LS10). The open circles indicate trace elements ($\times10^{-6}$); the black circles indicate invariable elements (%).

(2) The component migration of fine granite (LS18) to gneissic mylonite (LS15) can be found according to Table 4 and Fig. 3. Under Al_2O_3 conservation, $m_o/m_A = 0.896$, about the same as the iso-proportion line, $C_i = 0.896\ C_i^o$. The bring-in of Fe_2O_3, FeO, SiO_2 and K_2O is evident in the gneissic mylonite, Y and Mo are increased in trace elements (Fig. 3).

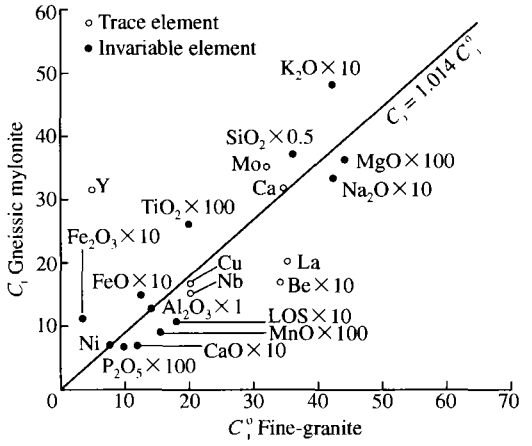

Fig. 3. Mass iso-proportion line of gneissic mylonite in ductile shear zone—the proportion of gneissic mylonite (LS15) with fine granite (LS18).

(3) The component migration of gneissic my-

lonite (LS15) to mylonite (LS13) can be found in Table 4, same as the above-mentioned facts, $m_o/m_A = 1.017$, about the same as the iso-proportion line of $C_i = 1.017$. Considering that the gneissic mylonite and mylonite can be classified into the same category, their symbolic elements brought in and out are not as evident as those of the above two cases.

2 Distribution of trace elements

Due to the fact that little work was done before in this aspect, the trace elements are listed independently in this paper, studied along with the major components, though the trace elements are contained as secondary components in the solid solution of major components in shear zones (Table 1). Besides analyzing the samples in the shear zones of the Xingzi area (Table 2), systematic correlative testing is also carried out for the trace elements in the shear zones of metamorphic core complex in the neighboring Wugongshan for comparison (Table 5). It is not difficult to find that there are distinct characteristics from the center to the margin of the ductile shear zones. Four series are about to be divided: assemblage component (element), divergence component, isotropic component and metallogenic component[10-12].

Table 5. Trace element abundances ($\times 10^{-6}$) from tectonites in ductile shear zone of the Wugongshan metamorphic core complex, northern Jiangxi[a]

Element	SZ-1 Giant grained granite	SZ-2 Coarse granite	SZ-3 Medium-fine granite	SZ-8 Fine granite	SZ-4 Gneiss	SZ-5 Mylonitic gneiss	SZ-12-1 Mylonitic gneiss	SZ-12-2 Gneissic mylonite	SZ-12-3 Mylonite	SZ-14 Mylonite	SZ-16 Proterozoic quartz schist	SZ-18 Proterozoic mica schist
Sr	115.32	124.52	105.68	65.68	165.42	150.40	61.60	105.34	205.24	93.16	557.04	374.64
Pb	28.04	93.54	76.07	121.42	28.59	15.14	511.30	29.83	30.02	32 26	21.02	203.74
Zn	78.44	87.76	82.30	73.32	119.28	129.46	204.50	116.02	124.50	106.12	84 76	181.60
Cu	24.68	9.16	14.34	12.04	13.30	30.20	116.96	20.42	30.22	79.38	70.44	12.90
Rb	821.40	421.00	232.20	446.80	570.80	458.80	773.80	449.40	797.20	457.60	137.96	638.40
Cr	70.70	28.40	25.40	40.30	59.80	183.06	154.12	187.34	136.00	59.56	313.50	274.50
V	22.00	34.12	38.22	11.22	105.44	125.28	87.64	56.12	69.36	17.32	17.96	177.06
Be	2.60	3.94	4.84	0.93	2.68	2.46	5.42	1.37	2.53	2 06	5.00	1 42
Co	4.22	5.55	6.46	2.66	12 75	20.11	12.05	10.57	14.07	4.68	4.93	37.52
Ga	13.90	15.33	16.30	13.55	18.19	14.63	17.44	13.56	14.40	20.58	14.85	13.62
Li	39.74	63.65	74.70	32.29	55.87	64.69	83.32	69.26	60.22	32.06	6.90	51.79
Mn	715.96	681.19	984.55	507.28	992.74	1303.92	805.62	793.14	853.98	489.79	650.31	1223.56
Mo	0.62	0.44	0.58	0.50	0.57	0.63	0.74	0.69	0.63	0.81	0.89	0 59
P	333.88	595.51	835.57	522.61	956.29	587.90	485.35	573.48	539.46	161.11	1695 52	583.52
Ni	8.62	3.60	5.59	3.14	6.72	19.21	24.14	24.06	28.67	8.70	12.78	90.77
Sc	7.18	6.42	7.36	3.04	13.68	20.20	16.22	9.62	10.84	7.80	5.68	27.98
Sn	19.92	19.76	22.28	12.64	25.90	27.52	26.22	21.87	20.12	15.36	16.17	22.30
Ti	1276.06	2869.46	3241.46	1647.86	5105.46	3625.46	4121.46	3859.46	4041.46	1314.46	1315.46	2541 46
Cd	0.002	0.20	0.002	0.002	0 26	0.34	0.04	0.22	0.002	0.002	0.44	0.32
La	25.58	50.24	48.14	57.06	63.80	34.92	37.10	51.84	12.24	25.32	15.02	22.94
Ce	65.96	87.76	82.30	106.70	111.42	58.82	64.60	88.74	56.42	85.12	30.12	43.58
Yb	2.36	2.22	2.96	1.16	2.14	4.14	0.90	1.28	1.26	4.36	3.20	3.40
Y	13.50	21.24	22.50	12.04	24.40	23.56	11.12	14.06	7.64	27.88	16.44	17.20

a) Analyzed by Qi Liang, Open Laboratory of Ore Deposit Geochemistry, Institute of Geochemistry, Chinese Academy of Sciences, Guiyang.

(1) Assemblage component series. Y, Yb and Be of trace elements and Si, Fe and Mg of major elements reveal a stable accumulation in the shear zones (Figs. 2 and 3). The content of Be in sample LS14 (Table 2) is about fifty times higher than that in sample LS10 of the country rock (Fig. 4). It is concluded that these elements are jointly characteristic of small ion radius, big specific gravity and high potential[10,11].

(2) Divergence component series. Ba, Sr and Rb of trace elements and Na and other elements of major elements all show the divergent and lost features in the center of the ductile shear zones (Figs. 2 and 3). The content of Ba in Sample LS16 (Table 2) is much lower than that in Sample LS10 of the country rock (Fig. 5). Contrary to the above case, big

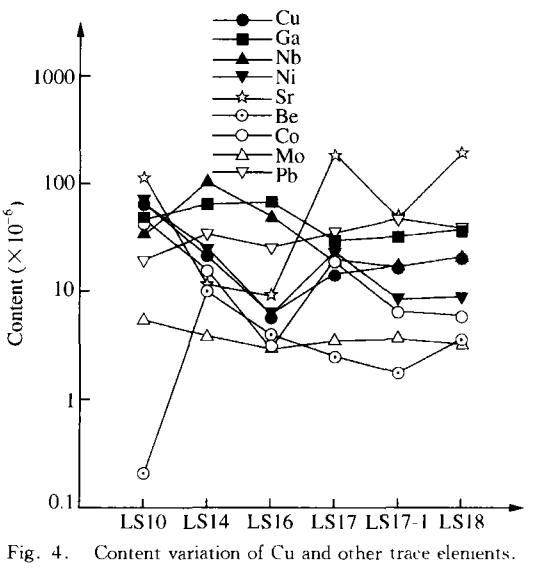

Fig. 4. Content variation of Cu and other trace elements.

ion radius, small specific gravity and low potential are the common features for these elements.

(3) Isotropic component series (aka uniform component series). The isotropic behavior of the elements Ti, Sn and Mo is rather evident (Tables 1 ~ 5). The latter differs little in its maximum (0.99) and minimum (0.50) values in the shear zones.

(4) Metallogenic component series. The metallic elements like Cu, Pb and Zn exhibit distinctions (Table 4), and the content of Cu is about 5 ~ 10 times higher than that in granite and mica schist of the country rocks. The major geochemical parameters and ion radius for the elements like Cu are similar to those of the elements in the assemblage component series.

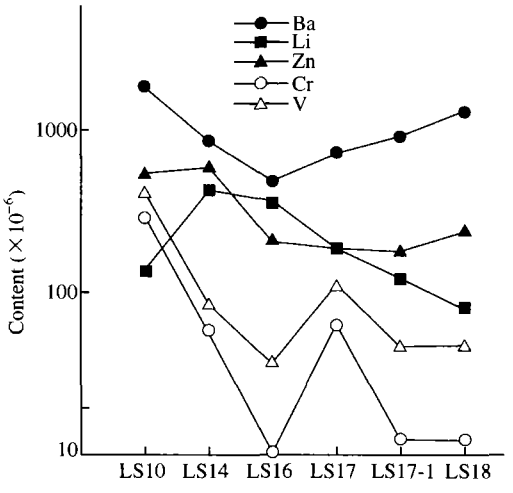

Fig. 5. Content variation of Ba and other trace elements.

3 Partitioning of rare earth elements

There are similarities among the chemical properties of rare earth elements. However, within the individual element, there are small differences in the respect of crystal chemistry (such as ion radius, electrovalence, etc.). Because of the small differences, the REE in the process of fault tectono-geochemical mechanism is very sensitive and easily identified. In correlation with rock-forming elements, the trace elements exhibit an evident traceable character that can be analyzed from the following four aspects[13,14].

(1) In the analysis of the samples in Tables 1 ~ 3, from the country rocks to the ductile shear zones (regardless of fine granite or mica schist), the bulk volume (ΣREE) of the rare earth elements reveals an increasing trend except sample LS16, and sample LS14 is 3 times as much as the sample LS10.

(2) The ratio of heavy and light rare earth elements (HREE/LREE) reveals accumulative properties on the surface of the granite side in the ductile shear zones; contrary properties are shown on the mica schist side. In fact, the ratio of concentration value of La/Y also reflects the above phenomena.

(3) The partitioning curves of the rare earth elements exhibit particular characters (Fig. 6). The partitioning curve of LS18 of the country rock dips rightward, and the partitioning curve of LS10 is as flat as bee-line. The curves for the rest samples dip gently towards the right, and rise from Gd-Y with Eu as the turning point. Though the curves keep the basic patterns of the original partitioning model, the rising curves for mylonite samples are more outstanding, and the three highs are formed at Tb, Tm and Lu (Fig. 6).

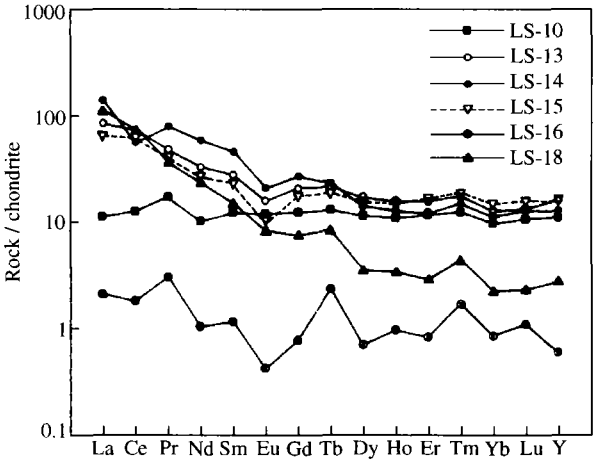

Fig. 6. The partitioning curves of the rare earth elements in Table 3.

(4) Eu anomaly is calculated by taking the chondrite normalized value, the primary rock tends to be normal, while the gneissic mylonite and mylonite show a moderate negative anomaly of E_u ($E_u/E_u^* = 0.430 \sim 0.649$).

4 Three kinds of correlations

The distribution phenomena, behavior mechanism of the trace elements and rare earth elements in the ductile shear zones of the metamorphic core complex can be explained by the following three tectono-geochemical mechanisms.

4.1 Rock rheologic differentiation

Rheologic differentiation is the most direct representation of the dynamic and metamorphic differentiations of the rocks. So the particle size of gneissic mylonite and mylonite turns finer when it approaches the schist, and becomes coarser-grained when it approaches the granite. Whereas their commonness lies in the major elements, trace elements and rare earth elements listed in Tables 1～4, and differentiation is the cause of the division of the assemblage and divergence component series based on the parameters of radius, specific gravity and potential of the different elements. Without doubt, the stress plays a dominant role, and the rock produces a distinct horizontal zoning of ductile and slipping rheology (Fig. 1) and facilitates the progressive increase or decrease of the elements (Table 1, Figs. 4 and 5)[10,11].

4.2 Coupling of mechanics and chemistry

Basically, rock rheologic differentiation is a variation of solid solutions, while the coupling of mechanics and chemistry mainly represents the penetration and diversion of the liquid fluid[15,16], whose cases are more changeable. In the ductile shear zones, the fluid activity, water-rock reaction and self-organizing function correlate directly with the dynamic pumping pressure[17,18]. Thermo-mechanical, coupling of mechanics and chemistry turn more active because of the penetration of fluid, resulting in the production of silica-rich system in dynamic metamorphic rocks (shown even in the plastic deformed domains of the brittle fault walls) and the increase of acid plagioclase (optical remarkable for the former, see Table 1). Under such conditions of geochemistry and rocks and minerals, ΣREE is easy to be enriched, Eu is easy to be lost, and traceable role is able to be played for the metallic mineralization[13,19].

4.3 Inversion of tectonic regime

According to the above analyses, the major elements, trace elements and rare earth elements in the ductile shear zones basically follow the rules of rheologic differentiation and chemical coupling. But in the respect of rare earth elements, HREE/LREE near the side of mica schist and ΣREE in sample LS16 vary out of harmony, especially the elements K and La that lined up first respectively in dissipation sequence of the major elements and rare earth elements. Close studies reveal that the phenomenon relates greatly with the inversion variation of tectonic regime from compressional type to extensional type of the ductile faults in the orogenic belts. Through ^{40}Ar-^{39}Ar age determination of stress minerals of the fault rocks, the conversion time in the region of Lushan is (104.4 ± 1.0) Ma[1)]. During this period, not only the feldspar mylonitic fabric presents a direct change[20], the deformability of the tectonic fault belts was strengthened and dynamic properties changed, but also two suites of utterly different water-rock reactions occurred: Dewatering-reduction series was transformed into hydrolysis-oxidation series[21]. As a result, the elements present a partial variation (especially on upside of the fracture) in the shear zones contrary to their overall distributions. Such a phenomenon is not difficult to be observed in the ductile shear zones[19,22].

In conclusion, through a systematic sampling test and mass equilibrium analysis of the three sorts of complex assemblages (intrusive complex, tectonic complex and metamorphic complex) and the analysis of all aspects of tectonogeochemistry, especially in trace elements and rare earth elements, in fault of ductile shear zone of metamorphic core complex, the authors find that, like major elements, the trace elements of small ion radius, big specific gravity and high potential like Y, Yb, Be, etc. form accumulative series in fault rocks, instead of divergence series like Ba, Sr, Rb, etc. in the trace elements. In rare earth elements, ΣREE is relatively centralized and the HREE/LREE is increased evidently. The partitioning curves rise from Gd-Y with Eu as the turning point and show a moderate negative anomaly of Eu. Only on the upside of the ductile fault, some phenomena contrary to the general rules are existent, most of which are restricted by the rock rheologic differentiation, coupling of mechanics and chemistry and inversion of tectonic regime.

References

1 Wernicke, B P. Low-angle normal faults in the basin and Range Province nappe tectonics in the extending orogen. Nature, 1981, 291: 645.
2 Malavielle, J P. Late orogenic extension in mountain belts: insights form the Basin Range Province the late Paleozoic Variscan belt. Tectonics, 1993, 12: 1115.
3 Zheng, Y. D. et al. Metamorphic core complex and extensional detachment fault in Neimenggu area. ACTA Geologica Sinica, 1993, 67: 301.

1) Detected by Prof. P. Monie, Isotopic Dating Laboratory, Montpellier University, France.

4 Sun, Y. et al. Study on the extensional tectonics and geodynamic evolution of the Wugongshan Area in the Jiangxi Province. Annual Science Report-Supplement of NJU(NS), 1994, 30: 69.
5 Michibayashi, K. Syntectonic development of strain independent steady-state grain size during mylonitization. Tectonophysics, 1993, 222: 151.
6 Shi, H. S. et al. The discovery of gold in quartz dislocation wall and its significance, Chinese Science Bulletin, 1994, 39: 322.
7 Davison, I. Laminar flow in shear zones: the Pernambuco Shear Zone, NE-Brazil. J. Struc. Geol., 1995, 17: 149.
8 Kisters, A. F. et al. Hydrologic segmentation of high-temperature shear zones: structural, geochemical and isotopic evidence from auriferous mylonites of the Renco mine, Zimbabwe. J. Struc. Geol., 2000, 22: 811.
9 Li, Y. C. et al. Tectonogeochemical features of middle part of Pangu-Bishui ductile shear zone in Heilongjiang Province, Chinese Journal of Geology, 2001, 36: 144.
10 Wu, X. Y. An Introduction of Tectonogeochemistry. Guiyang: Guizhou Science-Technology Press, 1998, 61: 355.
11 Sun, Y. et al. An Introduction of Tectonogeochemistry in Fault Zones (in Chinese). Beijing: Science Press, 1998, 33～73, 96～107.
12 Golubev, V. S. Thermodynamics of metasomatic mineral formation at mobile geochemical barriers during mass transport by infiltration. Int. Geochem., 1992, 20: 11.
13 Chen, J. et al. Distribution of REE and other trace elements in the Hetai deposit of South China: implications for evolutions an auriferous shear zone. J. Southeast Asian Earth Sci., 1994, 10: 217.
14 Albarede, F. Introduction to Geochemical Modeling. Cambridge: Cambridge University Press, 1995, 543.
15 Ouzegane, K. et al. Pressure -temperatrue-fluid evolution in E-burnean Metabasites and Metapelites from Tamanrasset (Hoggar, Algeria). J. Geol., 2001, 109: 247.
16 Hippler, S. J. Deformation microstructures and diagenesis in sandstone adjacent to an extensional fault: Implication for the flow and entrapment of hydrocarbons. AAPG. 1993, 77: 625.
17 Phyillips, J. D. Signatures of divegence and self-organization in soils and weathering profiles. J. Geol., 2000, 108: 92.
18 Sibson, R. H. Fluid pressure reductions induced by faulting their role as a precipitating agent at specific structural sites. SGEG, Ore Fluids Conference, Record (1990～1995), Canberra, Australia, 1991, 75～76.
19 Conti, A. et al. The relationship between evolution of fluid chemistry and the style of brittle deformation: examples from the Northern Apennines (Italy). Tectonophysics, 2001, 330: 103.
20 Prior, D. J. et al. Feldspar fabric in a greenschist facies albite-rich mylonite form electron backscatter diffraction (EBSD). Tectonophysics, 1999, 303: 29.
21 Sun, Y. et al. Two series of water-rock interaction in tectonic inversional regimes in the shallow level. J. Nanjing University (Geofluid Issue), 1997, 33: 53.
22 Zhou, J. B. et al. Application of REE anomaly in volume deficiency of a ductile shear zone—An example from the ductile shear zone on the northern margin of the Jiaonan orogenic belt. Geological Review, 1999, 45: 241.